Phase transition to spatial Bloch-like oscillation in squeezed photonic lattices

M. Khazaei Nezhad,[1] A. R. Bahrampour,[1] M. Golshani,[1] S. M. Mahdavi,[1,2] and A. Langari[1,3]
[1]*Department of Physics, Sharif University of Technology, Tehran 11155-9161, Iran*
[2]*Institute for Nanoscience and Nanotechnology, Sharif University of Technology, Tehran, Iran*
[3]*Center of Excellence in Complex Systems and Condensed Matter (CSCM), Sharif University of Technology, Tehran 145888-9694, Iran*
(Received 4 May 2013; published 1 August 2013)

We propose an exactly solvable waveguide lattice incorporating an inhomogeneous coupling coefficient. This structure provides classical analogs to the squeezed number and squeezed coherent intensity distribution in quantum optics where the propagation length plays the role of a squeezed amplitude. The intensity pattern is obtained in a closed form for an arbitrary distribution of the initial beam profile. We have also investigated the phase transition to the spatial Bloch-like oscillations by adding a linear gradient to the propagation constant of each waveguide (α). Our analytical results show that the Bloch-like oscillations appear above a critical value for the linear gradient of the propagation constant ($\alpha > \alpha_c$). The phase transition (in the propagation properties of the waveguide) is a result of competition between discrete and Bragg diffraction. Moreover, the light intensity decays algebraically along each waveguide at the critical point while it falls off exponentially below the critical point ($\alpha < \alpha_c$).

DOI: 10.1103/PhysRevA.88.023801 PACS number(s): 42.25.Bs, 42.82.Et, 42.25.Fx, 42.25.Hz

I. INTRODUCTION

Waveguide lattices provide an inexpensive experimental tool to study some physical phenomena in several branches of physics such as condensed matter, quantum optics, atomic, and molecular physics [1–6]. Nowadays these lattices can be realized by several methods such as optical induced technique, lithographic pattern, and laser writing methods [7,8]. In the weak coupling regime, the coupling strengths between adjacent waveguides can be adjusted by an appropriate change in the distance between guides [1]. Recently an exact solvable Glauber-Fock photonic lattice has been proposed in Refs. [9–12], in which the coupling coefficients are inhomogeneous and proportional to the square root of waveguide labels (assuming an incremental sequential label). These waveguide arrays provide an experimental tool to investigate interesting phenomena such as quantum random walk, photon bunching, and antibunching [10,12].

In the context of condensed matter physics, the energy levels of a superlattice form the Wannier-Stark ladders [5,13] when a constant external force is applied on its electrons. The extended Bloch wave function of electrons is converted to the localized Wannier states [5,13]. Moreover, the electrons show a periodic motion in these localized states, known as Bloch oscillation. Similar periodic motions have been observed for the light propagation in periodic waveguide arrays [14–18]. In such arrays the propagation direction plays the role of time, therefore the periodic motion is known as the spatial Bloch oscillations [14–18]. The effect of a constant external force can be simulated by exerting a linear transverse gradient on the propagation constants of the waveguide array [14–18]. To this end, the transverse temperature gradient in thermo-optical waveguides, transverse current in photorefractive waveguides, or a fixed curvature on a waveguide array during the fabrication process can be implemented [14–18].

In this paper we propose an exactly solvable semi-infinite optical waveguide lattice with inhomogeneous coupling coefficients. This array provides the classical analogs to the squeezed number and squeezed coherent intensity distribution in which the squeezed amplitude is proportional to the propagation length [19–22]. However, this is a classical simulation of the probability distribution of the squeezed state in the Fock space. Let us consider a cross section of the waveguide lattice as shown in Fig. 1, where each waveguide is corresponding to a state $(|n\rangle, n = 0, \ldots, \infty)$ in Fock space, i.e., $|n = 0\rangle$ represents the vacuum state. The occupation probability of each Fock state is given by the light intensity of the corresponding waveguide. The propagation of light within each waveguide (along the z direction) corresponds to the time evolution of the occupation probability of a Fock state. The squeezed number intensity distribution can be simulated classically by injecting a light beam into a single guide, while the Poisson distribution is applied to obtain the squeezed coherent intensity distribution.

We have also investigated the spatial Bloch oscillation in the proposed squeezed array. Surprisingly, we obtain the critical value of the strength of the linear gradient index to observe the Bloch-like oscillation ($\alpha \geqslant \alpha_c$). We discuss the long distance behavior of light intensity along the waveguides which shows three different behaviors, namely, exponential decay for $\alpha < \alpha_c$, algebraic decay at $\alpha = \alpha_c$, and Bloch oscillation for $\alpha > \alpha_c$. This oscillation comes from the interplay between discrete diffraction and Bragg diffraction. Here both the coupling coefficients and propagation constants are approximately proportional to the waveguide labels (n) which makes a competition between discrete diffraction and Bragg diffraction. Such a critical value does not exist in the Fock-Glauber and homogeneous lattices where the couplings are proportional to $\sqrt{n}$ and a constant, respectively, while the propagation constants are proportional to n which leads to the dominant Bragg diffraction and Bloch oscillation.

The paper is organized in four sections. Section II is devoted to the theoretical model and the exact solution which has been presented in our work. In Sec. III the spatial Bloch-like oscillation in the proposed waveguide lattices is investigated. Finally, we conclude and summarize our results in Sec. IV.

 ©2013 American Physical Society

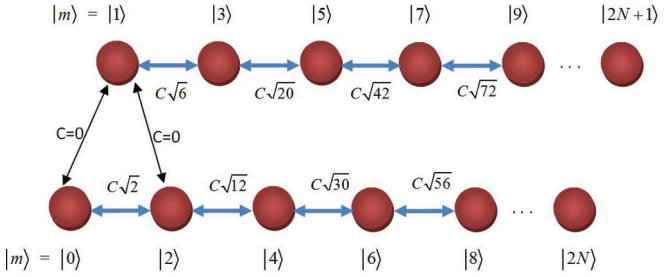

FIG. 1. (Color online) Cross section of the squeezed array of optical waveguides.

II. THEORETICAL MODEL

The nondegenerate squeezed operators depend on the square of annihilation and creation operators which prohibits the squeezed operators to be coupled to the even and odd Fock states simultaneously. Therefore, to simulate the squeezed states, as shown in Fig. 1, two different decoupled linear array of waveguides are taken into account. The upper waveguide array is labeled by odd numbers, while the lower array is labeled by even ones. The distance between the odd and even arrays of waveguides is large enough to decouple the odd and even waveguides, while the even-even and odd-odd nearest neighbor waveguides are coupled with nonzero coefficients. Although only one array (upper or lower) would be enough to simulate the vacuum squeezed and number squeezed states, both upper and lower arrays are necessary to be taken into account for simulating the coherent squeezed states, classically.

The slowly varying envelope approximation (SVEA) is implemented to write the light propagation equations in two linear waveguide arrays of Fig. 1. In this approximation the appropriate equations for light propagation in each waveguide is reduced to the common tight-binding (TB) model [1] as follows:

$$i\frac{dE_n(z)}{dz} + K_n E_n + C_n E_{n-2} + C_{n+2}E_{n+2} = 0, \qquad (1)$$

where E_n and K_n are the amplitude of the electric field and the propagation constant of the nth waveguide, respectively. In this section we consider identical waveguides and assume $K_n = K_0$. Moreover, C_n is the coupling coefficient between the nth waveguide and its preceding neighbor $n-2$. In the weak coupling regime, the coupling coefficients depend on the distance between neighboring waveguides such that $C_n = C_1 \exp[-\frac{d_n - d_1}{\kappa}]$, where C_1 and d_1 are the coupling coefficient and distance between the first coupled waveguides in the upper (odd labeled) or lower (even labeled) arrays, respectively. κ is a free parameter which is determined from coupled mode theory or experimental data [9,10,23]. In our model we assume that the coupling coefficients between even-even or odd-odd waveguide arrays are determined by $C_n = C_1\sqrt{n(n-1)}$ $(n > 1)$. It can be realized if we manipulate that the distance between waveguides is given by $d_n = d_1 - \frac{\kappa}{2}\ln[n(n-1)]$.

The new variables $Z = C_1 z$ and $E_n(z) = \Psi_n(Z)\exp(iK_0 Z)$ transform Eq. (1) to the following dimensionless form:

$$i\frac{d\Psi_n}{dZ}(Z) + \sqrt{n(n-1)}\Psi_{n-2}(Z) + \sqrt{(n+1)(n+2)}\Psi_{n+2}(Z) = 0, \quad n = 0,1,2,\ldots. \qquad (2)$$

In order to find the solution of Eq. (2), the following operator relation is defined:

$$i\frac{d\Phi}{dZ}(Z) = -(\hat{a}^2 + \hat{a}^{\dagger 2})\Phi(Z), \qquad (3)$$

in which $\Phi(Z) \equiv \sum \Psi_m(Z)|m\rangle$, where $|m\rangle$ represents the classical analogs of Fock states and denotes the optical mode of the mth waveguide. It will be shown that Eq. (3) is equivalent to Eq. (2) in terms of $\Psi_n(Z)$. The set $\{|m\rangle\}$ is called the waveguide number basis and $\Psi_m(Z)$ denotes the amplitude of electric field in the mth waveguide, which depends on the dimensionless propagation distance. $\hat{a}$ and $\hat{a}^\dagger$ are peculiar translation operators to the left and right, respectively, which are defined by $\hat{a}|m\rangle = \sqrt{m}|m-1\rangle$ and $\hat{a}^\dagger|m\rangle = \sqrt{m+1}|m+1\rangle$, similar to the bosonic annihilation and creation operators in quantum optics.

In terms of waveguide number basis, Eq. (3) is rewritten in the following form:

$$i\sum_m \frac{d\Psi_m(Z)}{dZ}|m\rangle = -\sum_m \sqrt{m(m-1)}\Psi_m(Z)|m-2\rangle - \sum_m \sqrt{(m+1)(m+2)}\Psi_m(Z)|m+2\rangle. \qquad (4)$$

The orthogonality of the waveguide number basis $(\langle m|k\rangle = \delta_{m,k})$ applied to Eq. (4) leads to

$$i\frac{d\Psi_k(Z)}{dZ} + \sqrt{(k+1)(k+2)}\Psi_{k+2}(Z) + \sqrt{k(k-1)}\Psi_{k-2}(Z) = 0, \qquad (5)$$

which justifies the equivalence of Eqs. (3) and (2). Therefore, it is sufficient to solve Eq. (3).

The solution of Eq. (3) can be written as

$$\Phi(Z) = \exp[iZ(\hat{a}^2 + \hat{a}^{\dagger 2})]\Phi(Z=0) = \hat{S}(-2iZ)\Phi(0), \qquad (6)$$

in which $\hat{S}(-2iZ)$ is the squeeze operator $\hat{S}(\xi) = \exp[\frac{1}{2}(\xi^*\hat{a}^2 - \xi\hat{a}^{\dagger 2})]$ with purely imaginary squeezing parameter $\xi = -2iZ$. The squeezed amplitude is twice the dimensionless propagation length and the squeezed phase is $-\frac{\pi}{2}$. By employing the disentangling theorem, the squeezed operator is given in the following form [21,22]:

$$\hat{S}(-2iZ) = \frac{1}{\sqrt{\cosh(2Z)}}\exp\left\{\frac{i}{2}[\tanh(2Z)]\hat{a}^{\dagger 2}\right\} \times \exp\{-\ln[\cosh(2Z)]\hat{a}^\dagger\hat{a}\} \times \exp\left\{\frac{i}{2}[\tanh(2Z)]\hat{a}^2\right\}. \qquad (7)$$

If we excite the waveguide array by injecting light beam at the nth waveguide, the amplitude of light in the lth waveguide at position Z along the propagation direction would be $\Psi_l^{(n)}(Z) = \langle l|\hat{S}(-2iZ)|n\rangle$. After some straightforward calculations, for even values of $|n-l|$, $\Psi_l^{(n)}(Z)$ can be written

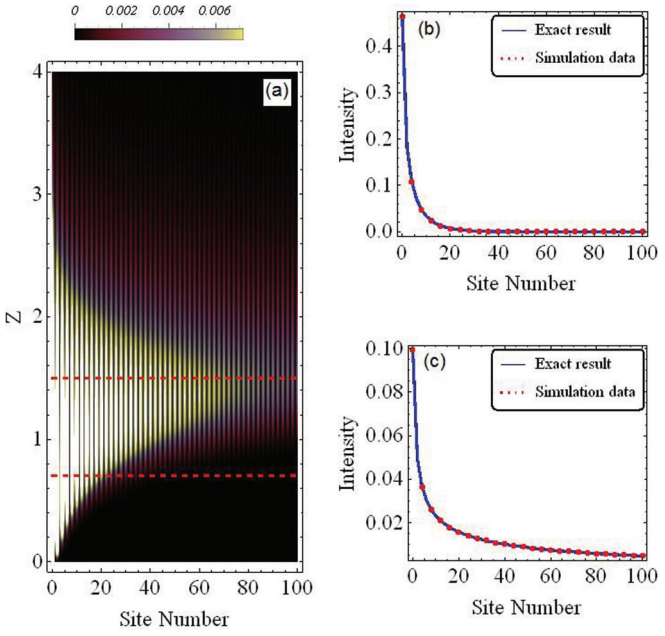

FIG. 2. (Color online) (a) Light intensity distribution for an initial excitation at $n = 0$. The light intensity profile versus site number at (b) $Z = 0.7$ and (c) $Z = 1.5$, solid lines are exact results and red circles comes from the Runge-Kutta-Fehlberg numerical simulation.

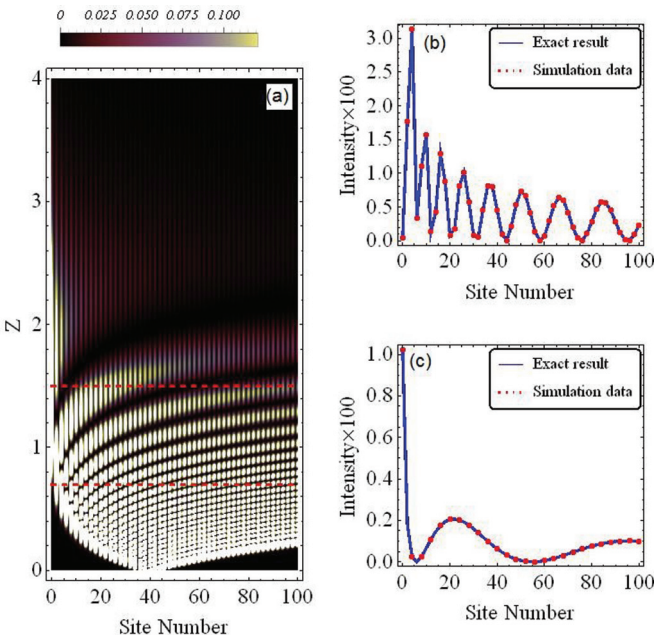

FIG. 3. (Color online) (a) Light intensity distribution for an initial excitation at $n = 20$. The light intensity profile versus site number at (b) $Z = 0.7$ and (c) $Z = 1.5$, solid lines are exact results and red circles comes from the Runge-Kutta-Fehlberg numerical simulation.

in the following closed form:

$$\Psi_l^{(n)}(Z) = \frac{\sqrt{n!\,l!}\left[\frac{-i}{2}\tanh(2Z)\right]^{\frac{n+l}{2}}}{\sqrt{\cosh(2Z)}} \times \sum_{m=0}^{M} \frac{(-2i)^{2m}}{[\sinh(2Z)]^{2m}[2m]!\left[\frac{l}{2}-m\right]!\left[\frac{n}{2}-m\right)]!}, \tag{8}$$

while $\Psi_l^{(n)}(Z) = 0$ if $|n - l|$ is equal to an odd number. Moreover, $M = \mathrm{Int}[\mathrm{Min}(\frac{n}{2}, \frac{l}{2})]$, where $\mathrm{Int}[x]$ means the integer part of a real number x.

The light intensity in the lth waveguide, at position Z along the propagation direction, is $I_l^{(n)}(Z) = |\Psi_l^{(n)}(Z)|^2$. The light intensity distribution is similar to the photon number distribution for squeeze number states versus time in quantum optics [19–22]. If light is injected in the first even labeled waveguide ($n = 0$), the light intensity distribution is similar to the squeezed vacuum photon distribution. For this case $M = 0$, and the light intensity distribution is reduced to the following form:

$$I_l^{(n=0)}(Z) = \frac{l!\left[\frac{-1}{2}\tanh(2Z)\right]^l}{\left(\frac{l}{2}\right)!\cosh(2Z)} \cos^2\left(\frac{l\pi}{2}\right). \tag{9}$$

Figure 2(a) shows the light intensity distribution in the lower (even labeled) array which is similar to the photon number distribution of the squeezed vacuum state. Figures 2(b) and 2(c) show the intensity versus even labels of waveguides at $Z = 0.7$ and $Z = 1.5$, respectively. To verify our analytical results, the system of Eq. (2) for 10 000 guides are solved numerically by the Runge-Kutta-Fehlberg method. The results of the numerical simulation have been shown by red circles in Figs. 2(b) and 2(c), which show perfect agreement with the exact (analytical) solutions.

Figure 3(a) shows the light intensity distribution when light is injected into an intermediate waveguide ($n = 20$) in the lower array, at the entrance plane. A reflection from the (fixed) left boundary is observed where the intensity is returned to the waveguides. The light intensity profiles are depicted at two different propagation lengths $Z = 0.7$ and $Z = 1.5$ in Figs. 3(b) and 3(c), respectively. These profiles show the oscillation of light intensity in the lower array of waveguides.

According to our study, $\Psi_l^{(n)}(Z)$ is interpreted as the impulse response for this structure. Therefore, for an arbitrary distribution of light intensity injected at the entrance plane, the light intensity distribution in each waveguide at the propagation distance Z is given by

$$\Psi_l(Z) = \sum_{n=0}^{\infty} \Psi_l^{(n)}(Z)\Psi_n(Z = 0). \tag{10}$$

If the intensity profile at the entrance plane is chosen to be a Poisson distribution such as $\Psi_n(Z = 0) = \frac{\beta^n}{\sqrt{n!}} \exp(-\frac{|\beta|^2}{2})$, where $\beta = |\beta|\exp(i\theta)$, the light intensity distribution at distance Z can be written as follows (for more details, see the Appendix):

$$I_n(Z) = |\langle n|\widehat{S}(-2iZ)|\beta\rangle|^2 = |\langle n|Z,\beta\rangle|^2 = \frac{\left[\frac{1}{2}\tanh(2Z)\right]^n}{n!\cosh(2Z)} \exp\{-|\beta|^2[1 + \sin(2\theta)\tanh(2Z)]\} \times \left|H_n\left[\frac{\beta}{\sqrt{-i\sinh(4Z)}}\right]\right|^2, \tag{11}$$

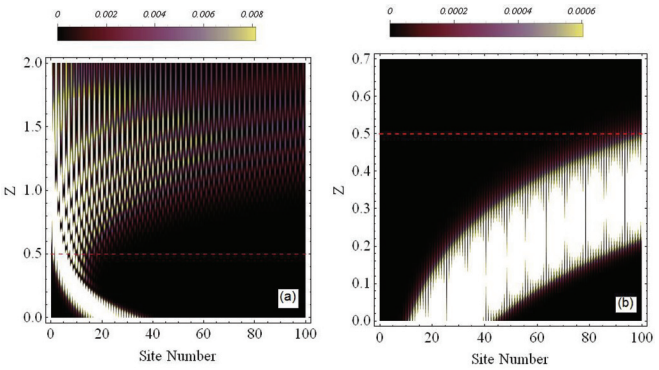

FIG. 4. (Color online) Light intensity distribution in the waveguide array along the waveguide length, for $N = 100, |\beta| = 4.0$, (a) $\theta = -\frac{\pi}{4}$, (b) $\theta = +\frac{\pi}{4}$.

where $H_n(x)$ is the Hermite polynomial of order n. The intensity profile of Eq. (11) is reminiscent of the squeezed coherent photon distributions.

Figure 4 shows the light intensity distribution along Z and versus the site number if a coherent light distribution is injected at the initial plane ($Z = 0$). Figures 4(a) and 4(b) present the light intensity distribution for two different phases of the initial light, namely, $\theta = -\frac{\pi}{4}$ and $\theta = +\frac{\pi}{4}$, respectively. These figures show that the reflection from the left boundary of the semi-infinite array can occur only for the negative initial phase.

The authors of Refs. [9,10] proposed waveguide lattices which provide the light intensity distribution for a coherent state by injecting an initial beam in the first guide of the lattice at the entrance plane. However, the interesting point of our work is to design a self-consistent structure implementing two different arrays to provide the squeezed coherent light intensity distribution. The squeezed coherent light distribution is established when the initial beam is exposed only to one of the waveguides at the entrance plane. This can be applied to classically simulate some phenomena related to the squeezed coherent states in quantum optics.

As mentioned before, if the exposing beam is applied on an even labeled waveguide, light propagates in the lower array, while an injection of light on the odd labeled waveguide, the propagation is on the upper array. The coherent state is a superposition of both even and odd states. For a coherent state, light propagates both in the upper and lower arrays. The intensity distribution would be similar to the photon distribution of the coherent squeezed state [19–22].

III. SPATIAL BLOCH OSCILLATION

In order to study the spatial Bloch oscillation in waveguide arrays, a linear transverse gradient is added to the propagation constants, i.e., propagation constants of waveguides are given by $K_n = K_0 + \Delta n$, where Δ is a constant. In the presence of the additional term (Δn), Eq. (2) is written in the following form:

$$i\frac{d\Psi_{\alpha,n}}{dZ}(Z) + \alpha n\Psi_{\alpha,n}(Z) + \sqrt{n(n-1)}\Psi_{\alpha,n-2}(Z) + \sqrt{(n+1)(n+2)}\Psi_{\alpha,n+2}(Z) = 0, \quad n = 0,1,2,\ldots, \tag{12}$$

where $\alpha = \frac{\Delta}{C_1}$. As shown for Eq. (2), the following equation is equivalent to Eq. (12):

$$i\frac{d\Phi}{dZ}(Z) = -(\hat{a}^2 + \alpha\hat{a}^\dagger\hat{a} + \hat{a}^{\dagger 2})\Phi(Z), \tag{13}$$

if $\Phi(Z)$ is expanded in the orthonormal waveguide number basis. The solution of Eq. (13) is

$$\Phi(Z) = \exp[iZ(\hat{a}^2 + \hat{a}^{\dagger 2} + \alpha\hat{a}^\dagger\hat{a})]\Phi(Z=0) = \hat{S}_\alpha(Z)\Phi(0), \tag{14}$$

where $\hat{S}_\alpha(Z)$ can be expressed in terms of SU(1,1) Lie generators. The generators are defined by $\hat{K}_+ = \frac{\hat{a}^{\dagger 2}}{2}$, $\hat{K}_- = \frac{\hat{a}^2}{2}$, and $\hat{K}_z = \frac{1}{2}(\hat{a}^\dagger\hat{a} + \frac{1}{2})$ which satisfy the following algebra:

$$[\hat{K}_+, \hat{K}_-] = -2\hat{K}_z; \quad [\hat{K}_z, \hat{K}_\pm] = \pm\hat{K}_\pm. \tag{15}$$

According to the structure of Lie algebra and employing the disentangling theorem we write $\hat{S}_\alpha(Z)$ as the product of three exponential forms [21]:

$$\begin{aligned}\hat{S}_\alpha(Z) &= \exp\left[-\frac{i\alpha Z}{2}\right]\exp[iZ(2\hat{K}_+ + 2\hat{K}_- + 2\alpha\hat{K}_z)] \\ &= \exp\left[-\frac{i\alpha Z}{2}\right]\exp[\phi(Z)\hat{K}_+]\exp[\phi_z(Z)\hat{K}_z] \\ &\quad\times \exp[\phi(Z)\hat{K}_-],\end{aligned} \tag{16}$$

where

$$\begin{aligned}\phi(Z) &= \frac{-2\sinh(\Gamma Z)}{i\Gamma\cosh(\Gamma Z) + \alpha\sinh(\Gamma Z)}, \\ \phi_z(Z) &= -2\ln\left[\cosh(\Gamma Z) + \frac{\alpha}{i\Gamma}\sinh(\Gamma Z)\right].\end{aligned} \tag{17}$$

Here $\Gamma = \sqrt{4-\alpha^2}$ which is real for $\alpha < 2$ while it is purely imaginary for $\alpha > 2$.

The light intensity in the lth waveguide at position Z, when the array is excited by an input at the nth waveguide, is given by $I_l^{(n)} = |\langle l|\hat{S}_\alpha(Z)|n\rangle|^2$, and can be obtained by employing the normal form factorized evolution operator [Eq. (16)]. More insight on the product form of $\hat{S}_\alpha(Z)$ reveals that even (odd) waveguides are coupled to even (odd) ones. Because the SU(1,1) algebra confirms that the operation of $\hat{K}_+$ or $\hat{K}_-$ on an even (odd) state leads to another even (odd) state. Hence, the amplitude of light in the lth waveguide $[\Psi_{\alpha,l}^{(n)}(Z)]$ is obtained to be

$$\begin{aligned}\Psi_{\alpha,l}^{(n)}(Z) &= \langle l|\hat{S}_\alpha(Z)|n\rangle \\ &= \frac{\sqrt{i\Gamma(n!)(l!)}[-\sinh(\Gamma Z)]^{\frac{n+l}{2}}e^{-\frac{i\alpha Z}{2}}}{[\alpha\sinh(\Gamma Z) + i\Gamma\cosh(\Gamma Z)]^{\frac{n+l+1}{2}}} \\ &\quad\times\sum_{m=0}^{M}\frac{(-i\Gamma)^{2m}}{[\sinh(\Gamma Z)]^{2m}[2m]!\left[\frac{l}{2}-m\right]!\left[\frac{n}{2}-m\right)]!},\end{aligned} \tag{18}$$

for $|n-l| =$ even and $\Psi_l^{(n)}(Z) = 0$ whenever $|n-l| =$ odd. It is straightforward to show that the solution presented in Eq. (18) is reduced to Eq. (9) for $\alpha = 0$.

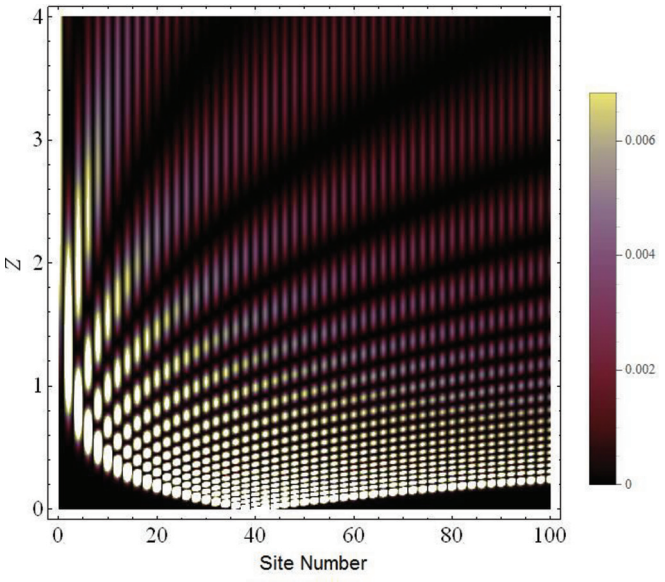

FIG. 5. (Color online) The profile of light intensity at the critical point $\alpha = 2.0$, where the initial beam is exposed at $n = 40$ for the semi-infinite array of waveguides.

For $\alpha < 2$, Γ is a real parameter, hence, the profile of light intensity is similar to what is presented already in Fig. 3 in the absence of linear transverse gradient in the propagation constants. If we concentrate our attention to the light propagation along the Z direction within a single waveguide, its long distance behavior is decaying exponentially, i.e., $I^{(n)}_{\alpha<2,l}(Z) \sim \exp(-\Gamma Z)$ for $Z \gg 1$. It is reminiscent of the overdamped behavior of the underlying system. However, for $\alpha > 2$, Γ is a purely imaginary parameter which will change the behavior of our system (as will be discussed). Therefore, we anticipate a phase transition at the critical parameter $\alpha_c = 2$.

At $\alpha = \alpha_c = 2$ the parameter Γ is zero which necessitates us to evaluate Eq. (18) in the limit $\Gamma \to 0$, we get

$$\Psi^{(n)}_{\alpha=2,l}(Z) = \frac{(iZ)^{\frac{n+l}{2}}\sqrt{n!l!}e^{-iZ}}{[1-2iZ]^{\frac{n+l+1}{2}}} \times \sum_{m=0}^{M} \frac{1}{[iZ]^{2m}[2m]!\left[\frac{l}{2}-m\right]!\left[\frac{n}{2}-m\right)]!}, \quad (19)$$

for $|n-l| =$ even and $\Psi^{(n)}_{l}(Z) = 0$ for $|n-l| =$ odd. The intensity profile at the critical point ($\alpha = \alpha_c$) is plotted in Fig. 5. The long distance behavior ($Z \gg 1$) of the intensity profile for any waveguide decays algebraically, i.e., $I^{(n)}_{\alpha_c,l}(Z) \sim \frac{1}{Z}$. This is the typical behavior at a critical point where fluctuations of all scales contribute to the phenomenon. Here the correlations decay algebraically which states that the diffraction exists on all length scales.

Nevertheless, for $\alpha > 2$, Γ is purely imaginary and the hyperbolic functions in Eq. (18) are converted to the periodic trigonometric functions where the spatial Bloch oscillation comes up. The spatial frequency of this oscillation is $Z_T = Cz_T = \frac{\pi}{|\Gamma|} = \frac{\pi}{\sqrt{\alpha^2-4}}$. Figure 6 shows the intensity pattern of this periodic propagation for $\alpha = 3.0$ for which the spatial frequency is $Z_T \cong 1.405$.

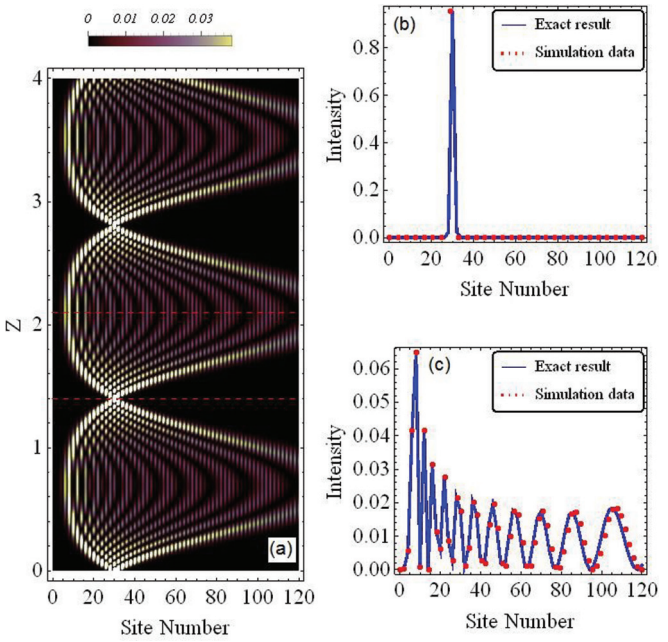

FIG. 6. (Color online) (a) Light intensity distribution of Bloch oscillation in the semi-infinite array of waveguides when the initial beam is exposed at $n = 30$ for $\alpha = 3.0$. The intensity profile versus site number at (b) $Z = 1.4$ and (c) $Z = 2.1$, solid lines are exact analytical results and red circles are the results of the Runge-Kutta-Fehlberg numerical simulation.

The spatial Bloch oscillation turns out from the interplay between discrete diffraction, Bragg diffraction, and surface reflection effects. In our model, due to the increase of the coupling coefficients by increasing the site numbers, discrete diffraction causes the expansion of light over large numbers of waveguides during propagation along waveguides. The role of Bragg diffraction appears when the phase differences between neighboring waveguides are equal to multiples of π. This condition can be satisfied at certain propagation lengths. At these points the expansion of light is terminated and light returns to the waveguides with lower propagation constants. Equation (12) shows that for high site labels ($n \gg 1$) both the coupling coefficients and propagation constants are roughly proportional to the site index n. Therefore, competition of discrete diffraction and Bragg diffraction causes the existence of a critical value for α. For α less than its critical value ($\alpha \leqslant \alpha_c$) the Bragg diffraction is suppressed by discrete diffraction, while for higher α ($>\alpha_c$) the Bragg diffraction is dominated. Moreover, the surface reflection causes repulsion at the $n = 0$ boundary. For $\alpha > \alpha_c$, Bloch oscillation occurs due to the reflection at high ($n \gg 1$) and $n = 0$ waveguides. Such a critical value does not exists in Fock-Glauber lattices where the coupling coefficients are approximately proportional to the square root of the site label ($\sqrt{n}$), while the propagation constants are proportional to the waveguide label (n). Hence, independent of how much the value of α is, the Bragg reflection is dominated and Bloch oscillation occurs.

$\Psi^{(n)}_{\alpha,l}(Z)$ is the impulse response for such structures. For an arbitrary distribution of light intensity injected at $Z = 0$, the light intensity distribution in each waveguides at propagation

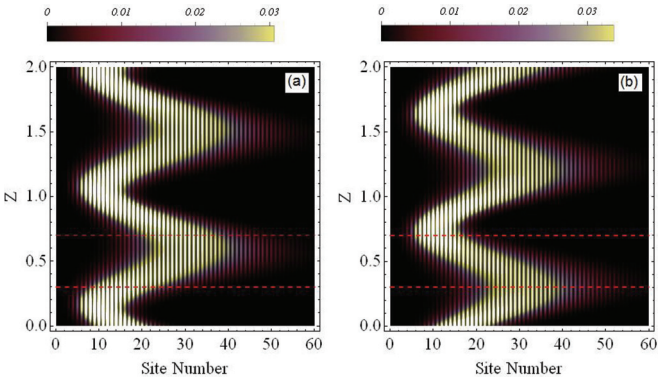

FIG. 7. (Color online) Light intensity distribution in waveguide array along the waveguide length, for $N = 60$, $\alpha = 4.0$, $|\beta| = 4.0$, (a) $\theta = -\frac{\pi}{4}$, (b) $\theta = +\frac{\pi}{4}$.

distance Z can be calculated as follows:

$$\Psi_{\alpha,l}(Z) = \sum_{n=0}^{\infty} \Psi_{\alpha,l}^{(n)}(Z)\Psi_n(Z=0). \tag{20}$$

If the light intensity distribution at the entrance plane is chosen from a Poisson distribution, i.e., $\Psi_n(Z=0) = e^{-\frac{|\beta|^2}{2}}\frac{\beta^n}{\sqrt{n!}}$, where $\beta = |\beta|e^{i\theta}$, the light intensity distribution at propagation distance Z can be written as follows (more details are presented in the Appendix):

$$\begin{aligned} I_n(Z) &= |\langle n|\widehat{S}_\alpha(Z)|\beta\rangle|^2 = |\langle n|Z_\alpha,\beta\rangle|^2 \\ &= \frac{\left|\frac{\nu'}{2\mu'}\right|^n}{n!|\mu'|}\exp\left\{-|\beta|^2\left[1+\mathrm{Re}\left(\frac{\nu' e^{2i\theta}}{\mu'}\right)\right]\right\} \\ &\quad\times\left|H_n\left[\frac{\beta}{\sqrt{2\mu'\nu'}}\right]\right|^2. \end{aligned} \tag{21}$$

Here $\nu' = \frac{2\nu}{\Gamma}$, $\mu' = \mu + \frac{\alpha\nu}{\Gamma}$, $\nu = -i\sinh(\Gamma Z)$, and $\mu = \cosh(\Gamma Z)$. We call $|Z_\alpha,\beta\rangle$ the generalized coherent squeezed states. Figure 7 shows the light intensity distribution for $\alpha > \alpha_c$, if the coherent light intensity distribution is injected at the $Z = 0$ plane. The spatial Bloch oscillation is easily seen in this figure. Figures 7(a) and 7(b) show the dependence of light intensity distribution on the initial phase of light.

IV. SUMMARY

We proposed the classical analogs of quantum *squeezed number* and *squeezed coherent states* in a semi-infinite lattice of waveguides with an appropriate tuning of the coupling coefficients. We have obtained the closed analytic form for the light intensity of any waveguide at position Z along its length, regardless of which waveguide has been exposed by an initial beam. The result has been extended to get the intensity profile for an arbitrary intensity distribution at the entrance of waveguides. Adding a linear gradient (α) to the propagation constant of the nth waveguide leads to a phase transition between two different behaviors. For $\alpha < 2$ we observed a pattern which comes from discrete diffraction similar to the $\alpha = 0$ case (Fig. 3), while for $\alpha > 2$ we observe the *spatial Bloch oscillation* in the array of waveguides (Fig. 6).

The nature of the phase transition is related to the interplay between discrete diffraction, which tends to expand the light over large numbers of waveguides, and Bragg reflection, which causes the light intensity to return to waveguides with lower propagation constants. Meanwhile, the reflection at the $n = 0$ boundary causes the light to return to the waveguides with increasing labels. Hence, an oscillation appears. We have also found the closed form of light intensity distribution, in the presence of linear gradient of refraction index, when a Poisson light distribution is chosen for the initial beam which is a classical simulation of generalized squeezed coherent states.

We propose that these fully integrable lattices provide new opportunities to study some interesting phenomena in quantum optics and condensed matter physics, such as *photon correlations* and *quantum phase transitions*, respectively. We have obtained the long distance ($Z \gg 1$) intensity profile which falls off exponentially for $\alpha < 2$ and an algebraic decay at the critical point $\alpha = 2$. This is similar to the spatial behavior of correlation functions in a magnetic system close to a quantum critical point. However, the observation and measurement of light intensity in an array of waveguides are much simpler than the corresponding counterpart in a magnetic system.

APPENDIX

In order to obtain Eqs. (11) and (21) we start with a more general case when $\alpha \neq 0$. For $\alpha = 0$, Eq. (21) can be converted to Eq. (11), so it is sufficient to get Eq. (21).

We define $\widehat{a}|0\rangle = 0$ which leads to

$$\widehat{S}_\alpha(Z)\widehat{D}(\beta)\widehat{a}\widehat{D}^\dagger(\beta)\widehat{S}_\alpha{}^\dagger(Z)|Z_\alpha,\beta\rangle = 0. \tag{A1}$$

Here we have defined $|Z_\alpha,\beta\rangle = \widehat{S}_\alpha(Z)\widehat{D}(\beta)|0\rangle$. The implementation of $\widehat{D}(\beta)\widehat{a}\widehat{D}^\dagger(\beta) = \widehat{a} - \beta$ leads to $\widehat{S}_\alpha(Z)\widehat{a}\widehat{S}_\alpha{}^\dagger(Z)|Z_\alpha,\beta\rangle = \beta|Z_\alpha,\beta\rangle$.

After some lengthy but straightforward calculations we obtain $\widehat{S}_\alpha(Z)\widehat{a}\widehat{S}_\alpha{}^\dagger(Z) = \mu'\widehat{a} + \nu'\widehat{a}^\dagger$. So,

$$\mu'\widehat{a} + \nu'\widehat{a}^\dagger|Z_\alpha,\beta\rangle = \beta|Z_\alpha,\beta\rangle. \tag{A2}$$

We expand the generalized coherent squeezed states in the Fock bases $|Z_\alpha,\beta\rangle = \sum_n C_n|n\rangle$. In these bases we arrive at the following relation:

$$\sum_n [\mu' C_n\sqrt{n}|n-1\rangle + \nu' C_n\sqrt{n+1}|n+1\rangle] = \gamma\sum_n C_n|n\rangle. \tag{A3}$$

We define $C_n \equiv \frac{N}{\sqrt{\mu'}}[\frac{\nu'}{2\mu'}]^{\frac{n}{2}} f_n(x)$, and replace it in Eq. (A3) which gives

$$\sqrt{n+1}\,f_{n+1} + 2\sqrt{n}\,f_{n-1} - \frac{2\beta}{\sqrt{2\mu'\nu'}}f_n = 0, \tag{A4}$$

Eq. (A4) is similar to the recursion relation of Hermite polynomials if we consider $f_n = \frac{1}{\sqrt{n!}} H_n(x)$ and $x = \frac{\beta}{\sqrt{2\mu'\nu'}}$. Thus, the expansion coefficients C_n can be written as

$$C_n = \frac{N}{\sqrt{n!\mu'}} \left[\frac{\nu'}{2\mu'}\right]^{\frac{n}{2}} H_n\left(\frac{\beta}{\sqrt{2\mu'\nu'}}\right), \tag{A5}$$

which gives $C_0 = \frac{N}{\sqrt{\mu'}}$. On the other hand, $C_0 = \langle 0|Z_\alpha,\beta\rangle$, which leads to $N = \sqrt{\mu'}\langle 0|Z_\alpha,\beta\rangle$. Moreover, we have

$$\langle 0|Z_\alpha,\beta\rangle = \frac{e^{-\frac{i\alpha Z}{2}}}{\sqrt{\mu'}} \exp\left[-\frac{|\beta|^2}{2} - \frac{1}{2}\beta^2\left(\frac{\nu'}{\mu'}\right)\right]. \tag{A6}$$

Therefore, by using Eqs. (A5) and (A6) for C_n, it is straightforward to reach Eq. (21).

[1] I. L. Garanovich, S. Longhi, A. A. Sukhorukov, and Y. S. Kivshar, Phys. Rep. **518**, 1 (2012).
[2] S. Longhi, Laser Photon. Rev. **3**, 3 (2009).
[3] F. Lederer, G. I. Stegeman, D. N. Christodoulides, G. Assanto, M. Segev, and Y. Silberberg, Phys. Rep. **463**, 1 (2008).
[4] D. N. Christodoulides, F. Lederer, and Y. Silberberg, Nature (London) **244**, 817 (2003).
[5] D. H. Dunlap and V. M. Kenkre, Phys. Rev. B **34**, 3625 (1986).
[6] A. Szameit, I. L. Garanovich, M. Heinrich, A. A. Sukhorukov, F. Dreisow, T. Pertsch, S. Nolte, A. Tünnermann, and Y. S. Kivshar, Nat. Phys. **5**, 271 (2009).
[7] T. Schwartz, G. Bartal, S. Fishman, and M. Segev, Nature (London) **466**, 52 (2007).
[8] Y. Lahini, A. Avidan, F. Pozzi, M. Sorel, R. Morandotti, D. N. Christodoulides, and Y. Silberberg, Phys. Rev. Lett. **100**, 013906 (2008).
[9] A. Perez-Leija, H. Moya-Cessa, A. Szameit, and D. N. Christodoulides, Opt. Lett. **35**, 14 (2010).
[10] R. Keil, A. Perez-Leija, F. Dreisow, M. Heinrich, H. Moya-Cessa, S. Nolte, D. N. Christodoulides, and A. Szameit, Phys. Rev. Lett. **107**, 103601 (2011).
[11] R. Keil, A. Perez-Leija, P. Aleahmad, H. Moya-Cessa, S. Nolte, D. N. Christodoulides, and A. Szameit, Opt. Lett. **37**, 3801 (2012).
[12] A. Perez-Leija, R. Keil, A. Szameit, A. F. Abouraddy, H. Moya-Cessa, and D. N. Christodoulides, Phys. Rev. A **85**, 013848 (2012).
[13] F. Bloch, Z. Phys. **52**, 555 (1929).
[14] G. Lenz, I. Talanina, and C. M. de Sterke, Phys. Rev. Lett. **83**, 963 (1999).
[15] T. Pertsch, P. Dannberg, W. Elflein, A. Brauer, and F. Lederer, Phys. Rev. Lett. **83**, 4752 (1999).
[16] R. Morandotti, U. Peschel, J. S. Aitchison, H. S. Eisenberg, and Y. Silberberg, Phys. Rev. Lett. **83**, 4756 (1999).
[17] F. Dominguez-Adame, V. A. Malyshev, F. A. B. F. de Moura, and M. L. Lyra, Phys. Rev. Lett. **91**, 197402 (2003).
[18] H. Trompeter, W. Krolikowski, D. N. Neshev, A. S. Desyatnikov, A. A. Sukhorukov, Y. S. Kivshar, T. Pertsch, U. Peschel, and F. Lederer, Phys. Rev. Lett. **96**, 053903 (2006).
[19] M. S. Kim, F. A. M. de Oliveira, and P. L. Knight, Phys. Rev. A **40**, 2494 (1989).
[20] C. Gerry and P. Knight, *Introductory Quantum Optics* (Cambridge University Press, Cambridge, 2005).
[21] R. R. Puri, *Mathematical Methods of Quantum Optics* (Springer, Berlin, 2001).
[22] D. F. Walls and G. J. Milburn, *Quantum Optics*, 2nd ed. (Springer, Berlin, 1994).
[23] A. Yarive, *Quantum Electronics*, 3rd ed. (Wiley, New York, 1989).